atmosphere

MDPI

Article

A Case Study of Drought during Summer 2022: A Large-Scale Analyzed Comparison of Dry and Moist Summers in the Midwest USA

Sarah M. Weaver [1,*], Patrick E. Guinan [1], Inna G. Semenova [2], Noel Aloysius [1,3], Anthony R. Lupo [1,3] and Sherry Hunt [4]

[1] Atmospheric Science Program, School of Natural Resources, University of Missouri, Columbia, MO 65211, USA; guinanp@missouri.edu (P.E.G.); aloysiusn@missouri.edu (N.A.); lupoa@missouri.edu (A.R.L.)
[2] Department of Military Training, Odessa State Environmental University, 65016 Odessa, Ukraine; in_home@ukr.net
[3] Missouri Climate Center, University of Missouri, 302 Anheuser Busch Natural Resources Building, Columbia, MO 65211, USA
[4] Agroclimate and Hydraulics Engineering Research Unit, United States Department of Agriculture—Agricultural Research Service, Stillwater, OK 74075, USA; sherry.hunt@usda.gov
* Correspondence: smfg2@missouri.edu; Tel.: +1-573-489-8457

Abstract: The summer of 2022 was very dry across Missouri and the surrounding regions including much of the Great Lakes, Midwest, and southern plains of the USA. A comparison of this summer to the dry summer of 2012 and the relatively wet summers of 2018 and 2021 was carried out using the National Centers for Environmental Prediction/National Centers for Atmospheric Research reanalysis, the Climate Prediction Center teleconnection indexes, and the blocking archive at the University of Missouri. The summer of 2022 was like that of 2012 which was characterized by a strong 500 hPa height anomaly centered over the western US and plains as well as very little blocking in the East Pacific. The summers of 2018 and 2021 were characterized by more zonal flow over the USA and more blocking in the East Pacific, similarly to the results of an earlier study. The teleconnection indexes for the prior spring and summer were largely similar for the two drier years and opposite for the wetter years. The surface conditions for the drier years were more similar while these were opposite for the wetter years. The integrated enstrophy (IE) used in earlier studies identified a change in the large-scale flow regime in early June 2022, which coincided with a decrease in the precipitation over the study region. However, one key difference was that the spring of 2022 was characterized by blocking more consistent with a wetter summer. This would have made the predictability of the drought of summer 2022 less certain.

Keywords: drought; blocking; teleconnections; integrated enstrophy; ENSO; long-range forecasting

Citation: Weaver, S.M.; Guinan, P.E.; Semenova, I.G.; Aloysius, N.; Lupo, A.R.; Hunt, S. A Case Study of Drought during Summer 2022: A Large-Scale Analyzed Comparison of Dry and Moist Summers in the Midwest USA. *Atmosphere* **2023**, *14*, 1448. https://doi.org/10.3390/atmos14091448

Academic Editor: Ognjen Bonacci

Received: 9 August 2023
Revised: 5 September 2023
Accepted: 6 September 2023
Published: 17 September 2023

1. Introduction

A drought is a typical ongoing issue during summer months for various parts of the United States; however, droughts can occur in any region of the world. The definition of a drought is a period that has abnormally dry weather sufficiently prolonged for the lack of water to cause serious hydrologic imbalance in an affected area (e.g., [1–3]). There are five different types of droughts that are categorized and defined based on what they affect. These five types of droughts include meteorological, agricultural, hydrological, socioeconomic, and ecological, and [3–8] (and references therein) describe the types of drought. Meteorological drought occurs when dry weather patterns dominate an area and evaporation exceeds precipitation (e.g., [5,7,8]). Hydrological drought occurs when low water supply becomes evident in the water system (e.g., [4,5]). Agricultural drought is associated with a lack of soil moisture in the root zone, which primarily affects crops due

to insufficient support for plant growth (e.g., [8]). Socioeconomic drought occurs when the supply and demand of various items become affected by drought (e.g., [6]). Ecological drought occurs when the natural ecosystem is affected by drought.

Short-term drought focuses on differences between precipitation and evaporation on the seasonal time scale (e.g., [4,9,10]), whereas these references describe long-term drought on a time scale of six months or greater. In addition, ref. [9] shows a trend toward more intense seasonal droughts in the Mediterranean over the last decade, while ref. [10] showed that longer term drought was forecast better in Peru using their technique.

Weather patterns that occur and relate to climatological conditions in disparate parts of the world are known as teleconnections, and these were defined as early as the mid-to-late 20th century (e.g., [11–13]). These common weather patterns and their variations will influence whether a region experiences such anomalies as hot and dry weather or wet and rainy conditions (e.g., [14–20] *and references therein*). These teleconnections have been found to result from Rossby wave propagation over a large region, and these can be driven by atmospheric dynamics as well as surface conditions (e.g., [20–23]). Studies such as [24,25] (*and references therein*) discussed or examined the impact of teleconnections, including drought, on agriculture. The work of [3] examined the linkage between teleconnections and droughts for the middle part of the United States and Eastern Europe/western Russia.

Integrated enstrophy (IE) can also be used as a measure for indicating a change in the Northern Hemisphere (NH) atmospheric flow regime or the onset or dissipation of blocking (e.g., [18,26–28]). Therein, ref. [29] examined IE for an entire year and determined that changes in IE could be related to changes in midwestern weather, and these changes could be anticipated one to two weeks in advance. The work of [18,30] discussed the possible use of IE to indicate seasonal changes. It is also important to note that east Pacific Region blocking can also be related to droughts and/or drought-like conditions over the middle part of North America (see, e.g., [16]).

In the United States, there have been severe droughts in years past particularly during the 1970s and since the 2010s as found in [3], with minima in the 1990s and 2000s. In this paper, a comparison is described of a recent severe drought summer (2012) with the non-drought years (2018 and 2021) for the Midwest United States (US) in order to determine if there was a common denominator using Northern Hemisphere teleconnections. Here, we will compare these summers with the recent drought year of 2022, which has not been studied yet. This work will examine whether blocking could have been used as an indicator for the drought of 2022. While this is not novel, this would provide support for earlier research. Also, IE is examined here in order to determine whether or not the start of the dry regime could be identified, and this has not been studied previously. Section 2 describes the materials and methods used. Section 3 will examine the large-scale atmospheric and surface conditions related to drought as in [3]. Section 4 will discuss the Midwest drought of 2022, and the last section will present the conclusions of this work.

2. Materials and Methods

2.1. Data

For this work, several data sources were used. The National Centers for Environmental Prediction/National Center for Atmospheric Research (NCEP/NCAR) reanalysis dataset was obtained via the website [31] to examine large-scale variables and to obtain the blocking characteristics. The NCEP/NCAR reanalyses are available on a 2.5 × 2.5-degree latitude/longitude grid and at 6-h intervals, but 1200 UTC data were used since these contain the most observations. This dataset is described in [32,33], has been assessed for quality by many (e.g., [34,35]), and has been used in numerous studies. These data have sufficient resolution for examining large-scale atmospheric phenomena and processes and over large study regions (e.g., [14–16]). Blocking events and the characteristics that are associated with each event are accessible on the University of Missouri archive [36]. This archive, the algorithms used, and the statistical character of blocking can be found in [37,38] and the references therein.

The primary upper air and surface variables used were 500 hPa geopotential height (m), surface precipitation rate (mm day^{-1}), and surface potential evaporation (E) (W m^{-2}). The potential evaporation data were converted to mm day^{-1} by dividing E by the latent heat of vaporization (L = 2.5 $\times$ 10^{6} J kg^{-1}) and the density of water (1000 kg m^{-3}), and 100 units of E are roughly 3.5 mm day^{-1}. This analysis will compare a severe drought season in the United States to wetter summers that occurred recently. For the United States, the years that were analyzed here were 2012, 2018, 2021, and 2022.

2.2. Study Region

The focal areas of this paper were that of the US as seen in Figure 1 and used in [3], and the box denotes the approximate study region outlined by 30° N to 50° N and 100° W to 80° W. These areas include much of the Midwest US and parts of the South and Northeast as seen in Figure 2. The primary dates consisted of the meteorological spring (1 March–31 May) and summer months (1 June–31 August), and the years chosen were 2012, 2018, 2021, and 2022.

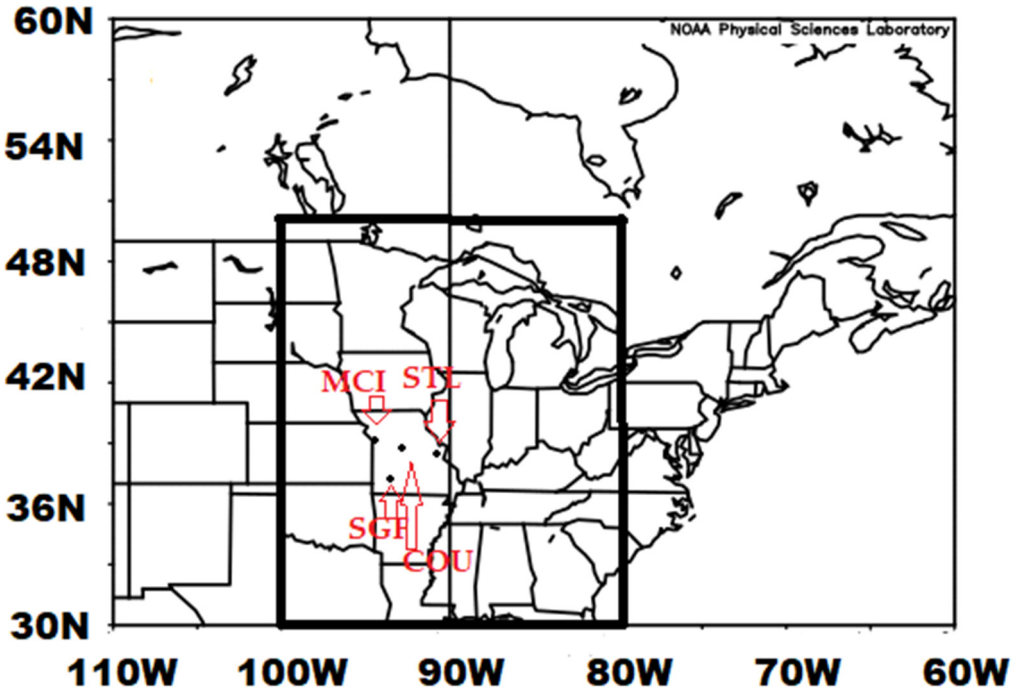

Figure 1. The study region in the US as defined by [3] and adapted from them. The three dots across the State of Missouri correspond to the National Weather Service Office locations for Kansas City (MCI), Columbia (COU), Saint Louis (STL) from west to east, and Springfield (SGF) in the Southwest.

2.3. Methodology

The methodology used in this analysis followed that found in [3] and is explained briefly here. In their work, the maximum E anomaly in mm day^{-1} was subtracted from the maximum negative precipitation anomaly to obtain a drought anomaly. The anomaly was modified by the percent of the study area covered by -1 mm day^{-1} or greater, which was estimated using box counts and the estimated error was +/− 0.02. In [3], severe drought was defined as a precipitation minus evaporation anomaly of -9.0 or greater. This work also examined the relationship with respect to the phase of El Niño and Southern Oscillation (ENSO) and the summer season transition. They also examined the preceding spring in order to determine whether or not drought was developing during the spring. This information is shown in Table 1. The years 2018 and 2021 did not count as drought years because of the small areas impacted. In this analysis, we will determine why precursors were not in favor of a drought for the summer of 2022 and the reasoning behind such.

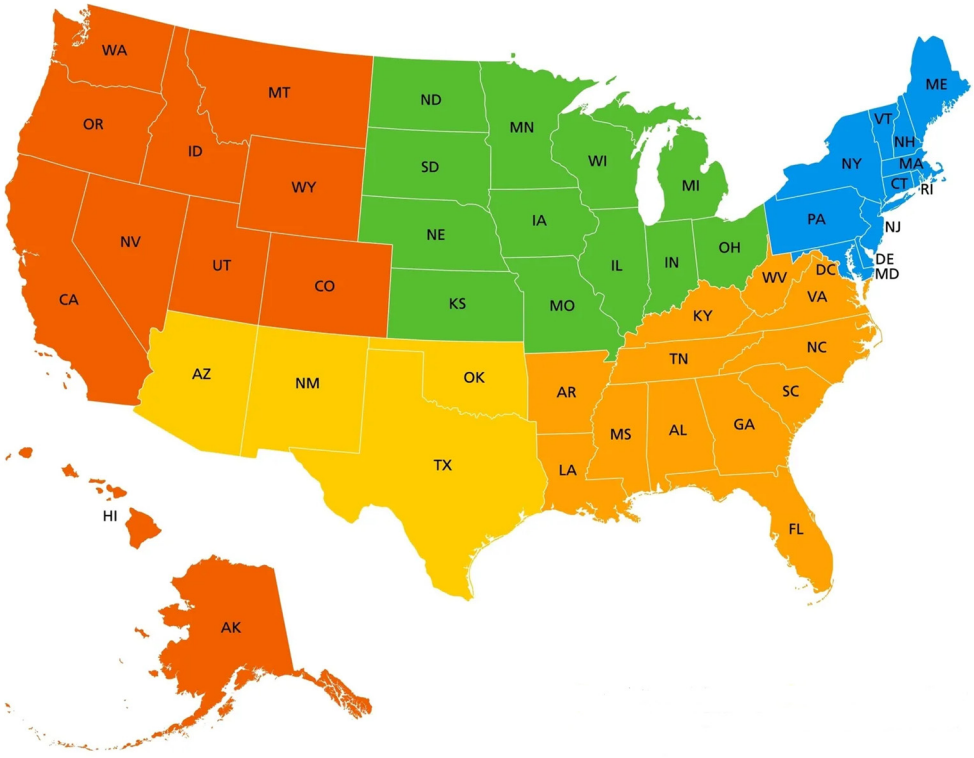

Figure 2. The sections of the US that include the West (deep orange color), Midwest (green color), South (light orange color), Southwest (yellow color) and Northeast (blue color) as defined by [39].

Table 1. From [3], the occurrence of extreme and moderate North American (NA) drought. Columns one, two, and three show the maximum precipitation minus evaporation anomaly (mm day^{-1}), the percent of the study region covered by -1 mm day^{-1} or greater P–E, and the product of columns two and three, respectively. Columns four, five, and six show the ENSO phase, as well as the type of ENSO transition taking place during the summer, and whether the preceding spring showed drought conditions, respectively. The estimated error in column 4 is +/− 0.1 to +/− 0.2 units.

Year	P–E Anomaly	%Area	Col. 2 × 3	ENSO Phase	Transition	Precursor
2012	−9.0	0.30	−2.7	NEU	NEU—NEU	Yes
2018	−6.6	0.10	−0.7	LA	LA—NEU	N/A
2021	−6.5	0.15	−1.0	LA	LA—LA	N/A
2022	−9.0	0.35	−3.2	LA	LA—LA	No

The definition used for blocking can be found in [26,27] and references therein, and this includes the algorithm for calculating BI which was based on 500 hPa height data. In calculating the integrated enstrophy (IE), we used the following equation:

$$\mathrm{IE} = \sum_{i>0} \lambda_i \approx \int_A \zeta^2 dA \quad (1)$$

where z is the 500 hPa vorticity and the value squared is enstrophy. The development and physical meaning of IE are discussed in [27] and the IE was calculated as in [28,30]. This value and the significance here will be discussed further in Section 4.

3. Results

3.1. Drought 2022 in Context: United States Statewide Ranks

Focusing on the summer months which include 1 June through 31 August 2012 and 2022, it is apparent that portions of the study region endured a drought, but 2018 and 2021 experienced much less over the same area (Table 1, Figures 3–7). Precipitation totals

were low for most of the Midwest, with temperatures being much above normal [40,41]. The years 2018 and 2021 were not drought years due to the lower (absolute) values of the drought index used here and shown in Table 1. In Figures 3–7 are shown the state-by-state ranks for temperature and precipitation for the summer season over an approximately 120-year period. Temperature (precipitation) is ranked from coldest (driest) (number one) to warmest (wettest). The comparison for the summer of 2012 versus 2022 in Figures 3 and 7 would indicate that 2012 was qualitatively worse when examining the ranks of temperature and precipitation. Further comparisons will be made below. Figure 4 demonstrates that the entire year of 2012 was among the warmest and driest for many of the states in the study region [39]. Most of the states had much above normal temperatures with eighteen states enduring record warmest temperatures for 2012 [42]. This indicates that the 2012 drought was persistent for much of the Midwest and portions of the South and West.

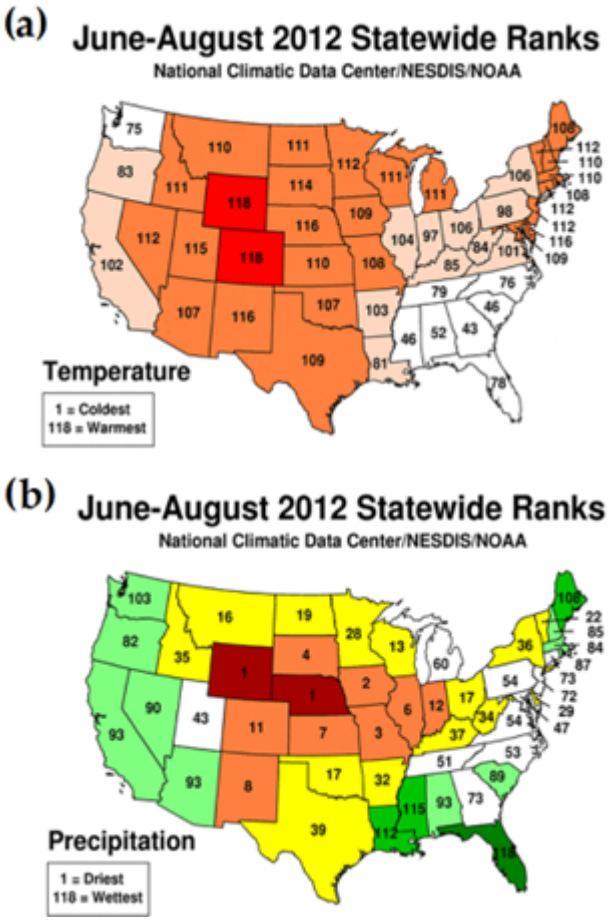

Figure 3. Statewide temperature and precipitation ranks for the United States during summer 2012 (Source: [40,41]). In (**a**), the dark red, orange, beige, white, light blue, medium blue, and dark blue indicate temperatures that were record warmest, much above normal, above normal, near normal, below normal, much below normal, and record coldest, respectively. In (**b**), the dark green, medium green, light green, white, yellow/light brown, medium brown, and dark brown indicate precipitation that was wettest, much above normal, above normal, near normal, below normal, much below normal, and driest, respectively. Temperature is on the left and precipitation, on the right. Ranks are such that the highest number indicates the warmest or wettest months, respectively.

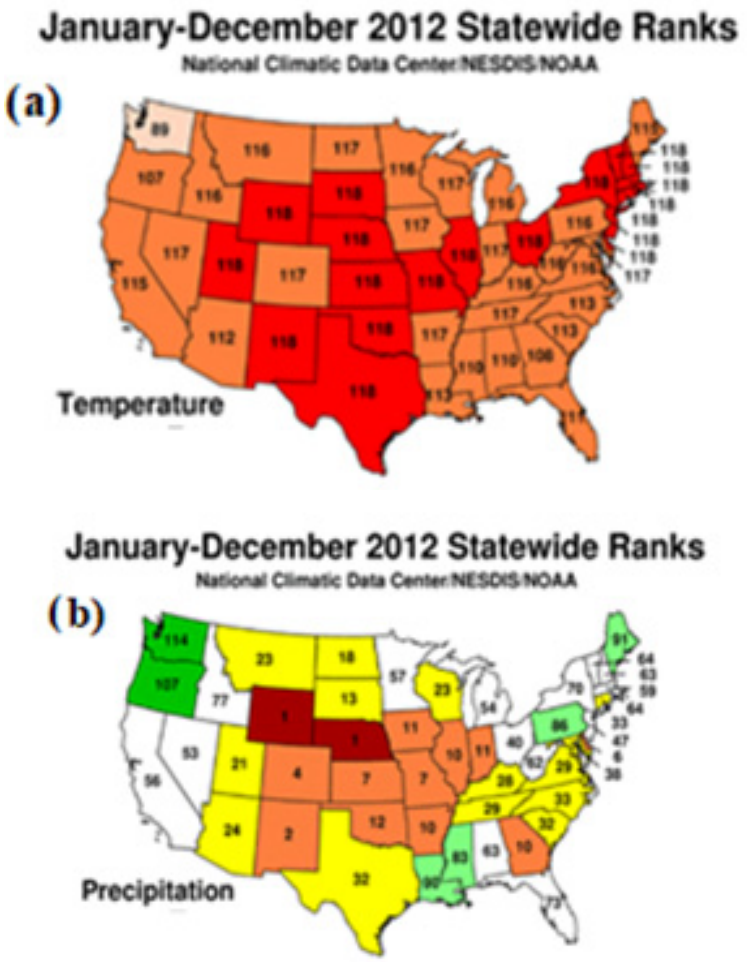

Figure 4. Statewide ranks for the United States for the entire year of 2012 showing both temperature and precipitation that occurred for the year [43,44]. Color schemes follow Figure 3.

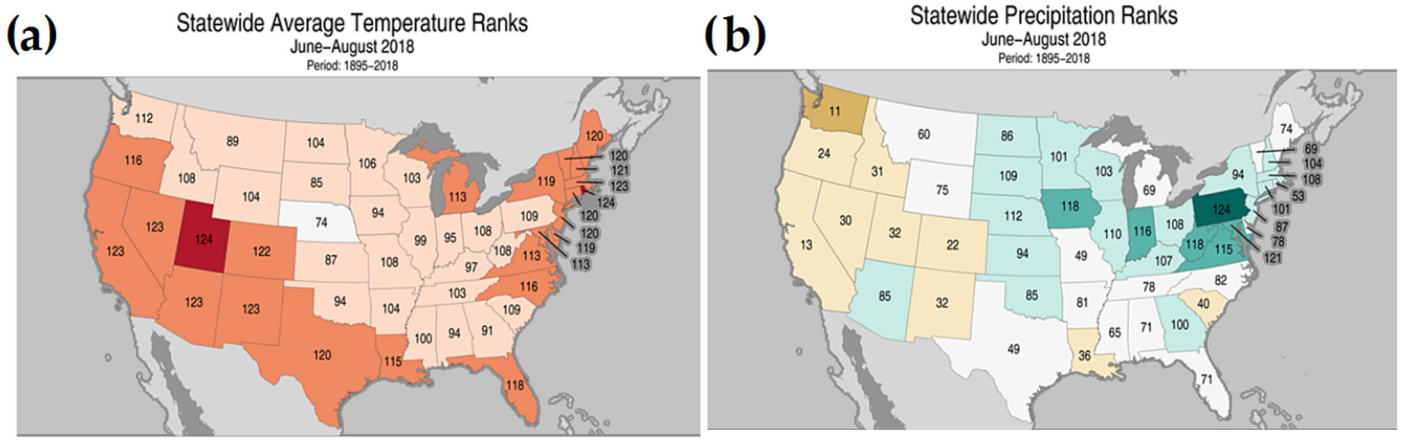

Figure 5. As in Figure 4, except for 2018. Source: [45]. Color schemes follow Figure 3.

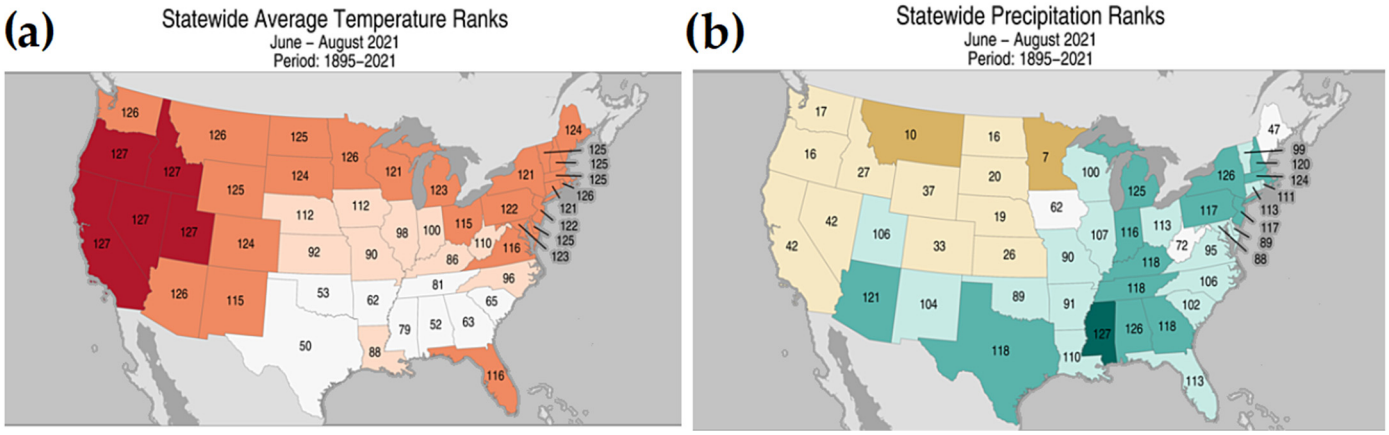

Figure 6. As in Figure 4, except for the year 2021. Source [46]. Color schemes follow Figure 3.

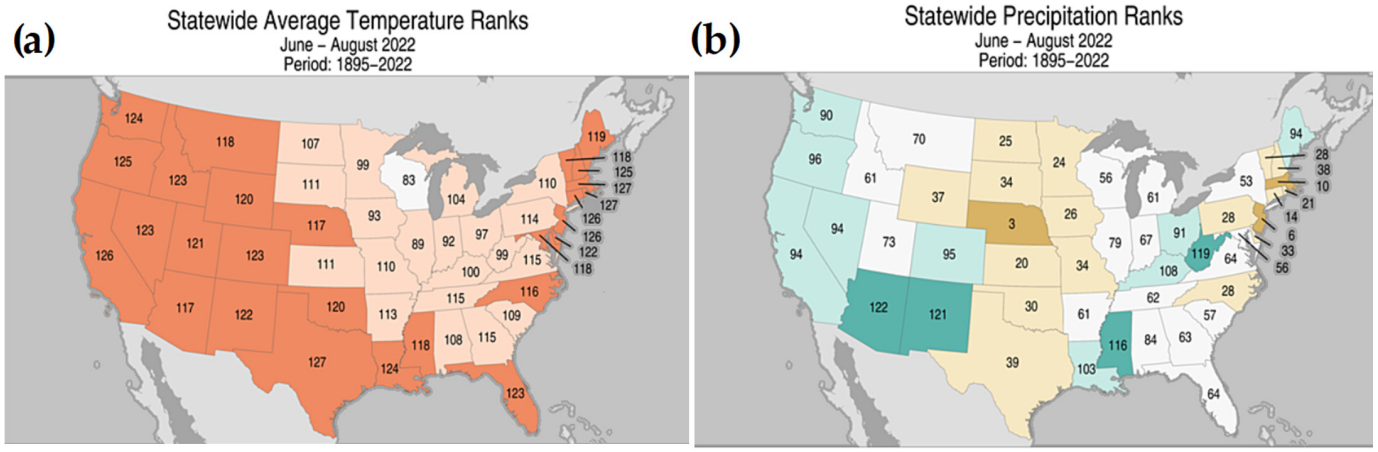

Figure 7. As in Figure 4, except for the year 2022. Source: [47]. Color schemes follow Figure 3.

Examining Figure 5, it can be deciphered that the Midwest endured temperatures that were much cooler during summer 2018 especially than that of the summer 2012, but still above normal. As for precipitation totals, areas that had above average precipitation were the states of North Dakota, Kansas, South Dakota, and Minnesota. As for the remainder of the Midwest including areas of Illinois, Indiana, Michigan, Wisconsin, Ohio, Iowa, and Nebraska, those areas had precipitation totals that were much above average.

The Midwest had temperatures that ranged from above average to much above average for the summer 2021 as seen in Figure 6. Missouri, Illinois, Indiana, Nebraska, Iowa, and Oklahoma were the states that had above average temperatures. However, Michigan, Ohio, Wisconsin, Minnesota, South Dakota, and North Dakota all endured temperatures that were much above average for the year 2021. Precipitation totals varied with Missouri, Illinois, Michigan, Indiana, Ohio, and the southern states being the states that had above average precipitation totals for the year 2021 as seen in Figure 6. However, Kansas through North Dakota and Minnesota had a lack of precipitation with precipitation totals being below average for the summer of 2021.

Temperature ranks for the Midwest and South during the summer of 2022 experienced mainly above average temperatures as seen in Figure 7. However, Oklahoma, Texas, Mississippi, and Louisiana had temperatures that were much above average. Precipitation totals varied for the Midwest for the year 2022 as seen in Figure 7. Nebraska was the only state in the Midwest that saw much below average precipitation totals. As for the other states in the Midwest, including Kansas, Iowa, Indiana, Minnesota, Missouri, and South Dakota, these areas had below average precipitation totals.

By July 2022 (Figure 8a), much of the study region was in the earlier stages of drought and this persisted into the summer and became more severe by mid-fall 2022 (Figure 8b). After November 2022, drought conditions slowly abated, but spring 2023 was very dry across the study region (not shown) and it could be argued that drought continues to persist.

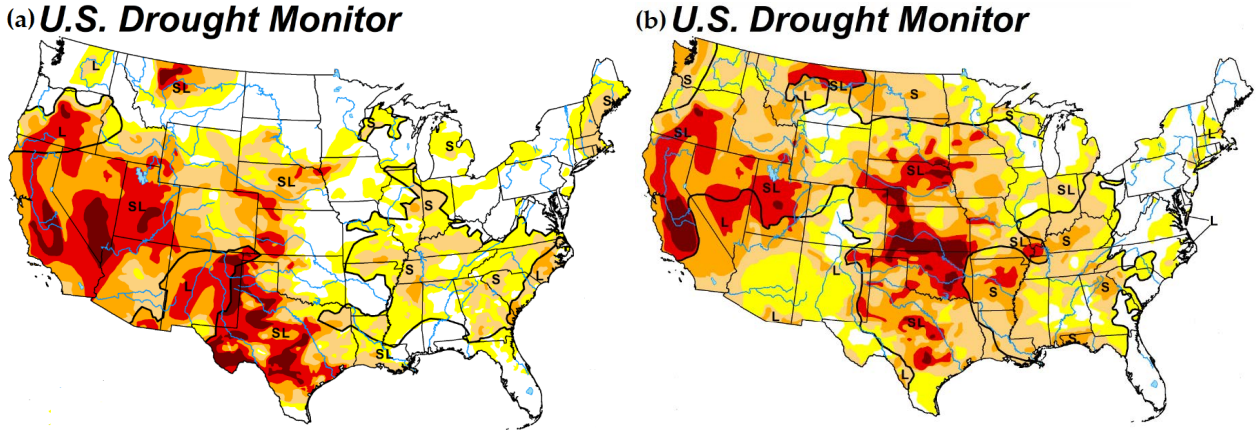

Figure 8. The US Drought Monitor maps for (**a**) 5 July 2022 and (**b**) 25 October 2022. Yellow (D0), beige (D1), orange (D2), red (D3), and dark brown (D4) correspond to abnormally dry, moderate drought, severe drought, extreme drought, and exceptional drought, respectively. Source: [48].

3.2. Teleconnections

A linkage was found by [3] between teleconnections and droughts over North America and Eastern Europe. The teleconnections examined were the Arctic Oscillation (AO), North Atlantic Oscillation (NAO), and Pacific/North American Pattern (PNA), and the data were obtained from [46]. The AO is a daily index that is projected daily at a height of 1000 mb height anomalies poleward of 20° N. The NAO is a daily index that shows anomalies for the North Atlantic region based on two centers of action. The PNA is another index that is used to describe the flow pattern over the Northeast Pacific region based on four centers of action. This index has been used in numerous studies to determine characteristic patterns of weather or climate cycles at different times of the year for North America. As mentioned in a previous study [3], blocking and teleconnections play an important role in determining and forecasting droughts and/or non-drought conditions for North America. The daily (Figure 9) values of these three indexes for 1 April to 30 June 2012 and 2022 are shown below, while the seasonal mean spring and summer values for all years studied here are shown in Table 2. These quantities will be discussed in Section 4; however, as demonstrated by [3,29,30], as well as previously by Lebedeva et al. [49], there is a high correlation between the daily AO and the NAO in 2012 and 2022 (0.46, 0.62/p = 0.01) (see Table 3) and a negative correlation between the AO and PNA (−0.23, −0.21/p = 0.05, 0.1, respectively) and NAO and PNA (−0.17, −0.26/the latter significant at p =0.05).

Table 2. Mean seasonal teleconnection index values that occurred during the spring/summer months for the years of study over the US [50].

Year	AO	NAO	PNA
2012	0.39/−0.15	0.28/−1.61	−0.05/−0.28
2018	0.26/0.61	0.81/1.48	−1.05/0.47
2021	0.58/0.42	−0.65/0.17	−1.12/0.73
2022	0.29/−0.08	0.37/0.42	−0.48/1.01

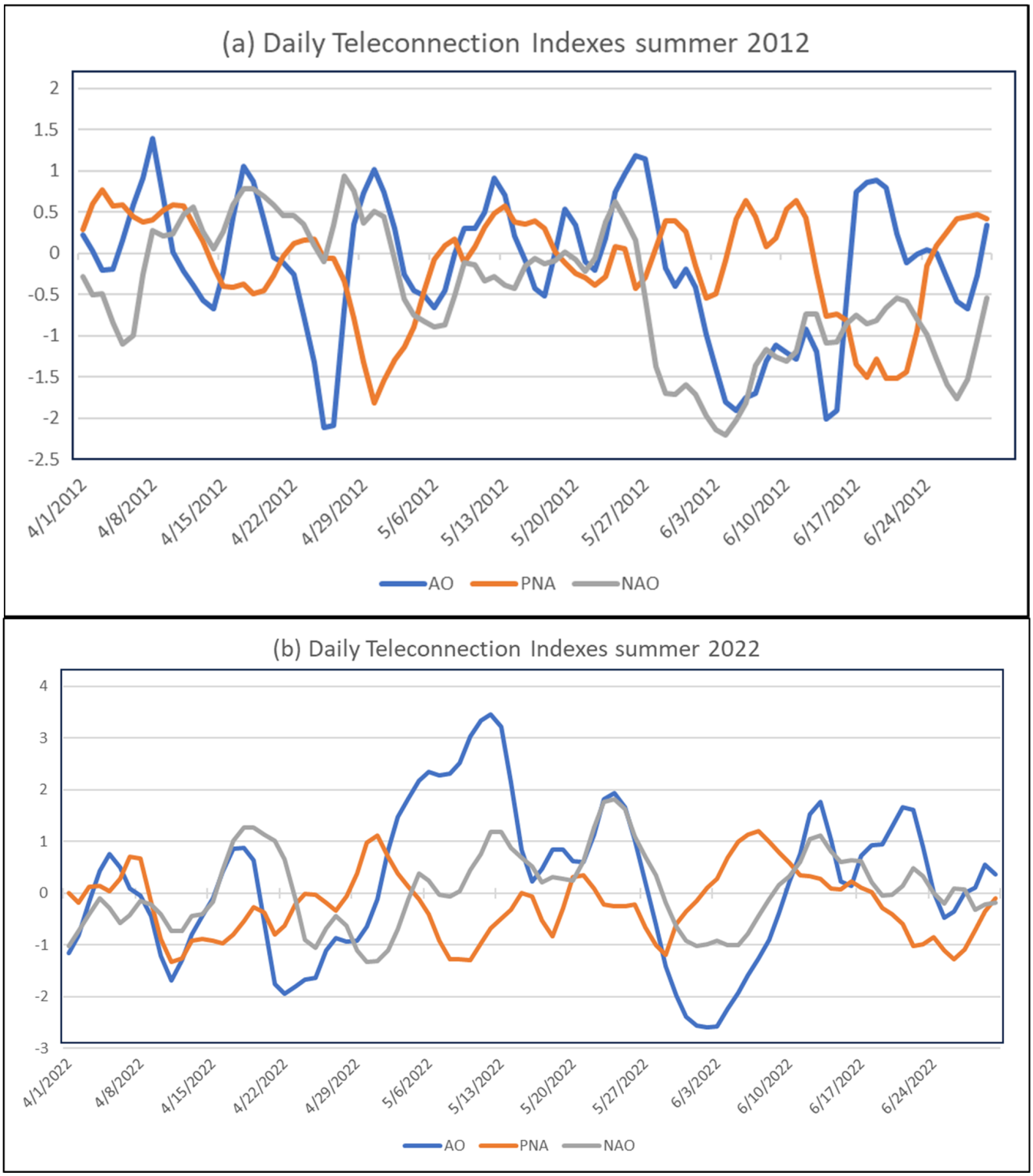

Figure 9. The daily teleconnection index values for the AO (blue), PNA (orange), and NAO (gray) from 1 April to 30 June, for (**a**) 2012, (**b**) 2022.

Table 3. Correlations of the daily teleconnection index values that occurred during the spring/summer months for the years of study over the US [50]. Correlations that are statistically significant at $p = 0.01$, $p = 0.05$, $p = 0.1$ are in bold red, blue, and green.

Year	AO/NAO	NAO/PNA	PNA/AO
2012	**0.46**	−0.17	**−0.23**
2018	**0.61**	**0.32**	**0.26**
2021	**0.65**	**0.49**	0.01
2022	**0.62**	**−0.25**	**−0.21**

3.3. 500 hPa Flow, IE, and Blocking—United States

Focusing on the US (Figure 10) for the 500 hPa height anomalies associated with the summer season (1 June through 31 August), the summer season 500 hPa height anomalies for 2012 and 2022 more closely resembled each other with positive anomalies over the western and central US. Conversely, the height anomalies of 2018 and 2021 were higher over southern Canada and the northern tier of states and lower over Northern Canada, implying a more zonal flow pattern over North America. Only the year 2012 was included in the composites in [3] and these will be discussed below.

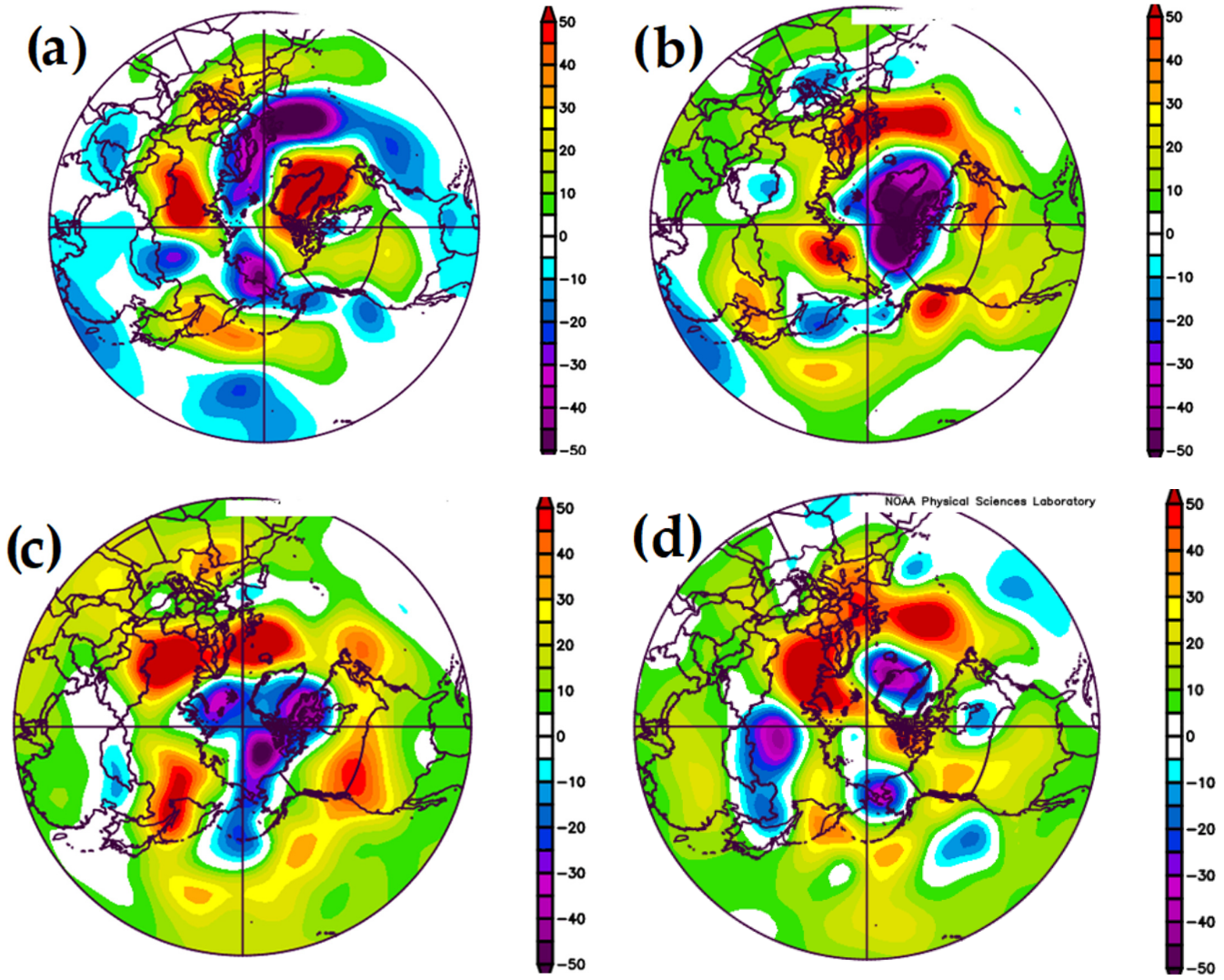

Figure 10. 500 hPa geopotential height (m) for the years (**a**) 2012, (**b**) 2018, (**c**) 2021, and (**d**) 2022; focused on the United States [31].

An examination of the spring and summer season blocking (Table 4) demonstrates results consistent with those found in [3], but also earlier studies such as [16,18]. The severe drought of 2012 was associated with no spring or summer blocking upstream of North America, consistent with the low 500 hPa height anomalies over the Gulf of Alaska and East Pacific (Figure 10a). A similar configuration is seen in Figure 10d. However, for 2022, the spring season was associated with six blocking events which is more consistent with a wet season. Then during summer 2022, there was only one weak blocking event (BI = 2.13 compared to mean event BI = 3.12—weak being about one standard deviation or more below the mean, see [36,38]), characteristic of dry summers.

Table 4. Blocking events occurring during the spring (March–May)/summer (June–August) months for the years of study over the Pacific Region 180° to 100° W in longitude.

Year	Blocking Events	Days	Block Intensity (BI)
2012	0/0	0.0/0.0	NA/NA
2018	1/2	9.0/14.0	4.24/2.69
2021	4/3	34.5/24.5	2.78/2.28
2022	6/1	52.5/20.5	3.00/2.13

The calculation of integrated enstrophy (IE) was conducted using a built-in computer programming code using Python. Again, as mentioned above, enstrophy is a conservative quantity in two-dimensional inviscid flow [51]. The NCEP-NCAR reanalysis [31] was used to obtain both the u and v wind components during the year 2022. These data were inputted into a Python code (see [30]). The works of [26–28] established that the local maxima in the IE were associated with a change in the large-scale flow regime over the NH as well as North America. This led to changes in the associated weather over the central part of North America [29,30], and [18,30] associated IE changes with a change in the seasonal character of temperature and precipitation regimes. Also, [29] showed that the IE has an annual cycle and the years 2012 and 2022 had a distinct annual cycle in IE (not shown), but only the period from 1 April to 30 June is shown here (Figure 11). The IE maxima in early June for both years will be discussed below.

Figure 11. Calculated integrated enstrophy (IE—km^2 s^{-2}) for 1 April to 30 June for the years (**a**) 2012 and (**b**) 2022. The red, blue, and yellow lines are the IE, 90-day mean IE, and one standard deviation from the mean, respectively.

3.4. Precipitation and Surface Potential Evaporation

Surface potential evaporation is the amount of water that could evaporate at the surface. More surface potential evaporation would equate to warmer temperatures and drought. The spring season precipitation and potential evaporation showed that during 2012 (Figure 12a,b), there was a shortfall of precipitation and excess potential evaporation in the Great Lakes within the study region as well as just west of the study region. In 2018 (Figure 12c,d) and 2021 (Figure 12e,f), respectively, the Southern Plains and Appalachian

regions were dry. In 2022 (Figure 12g,h), there was dryness in the Great Plains mainly west of the study region. Thus, during each year, there was potential somewhere in the eastern 2/3 of the US for a dry summer.

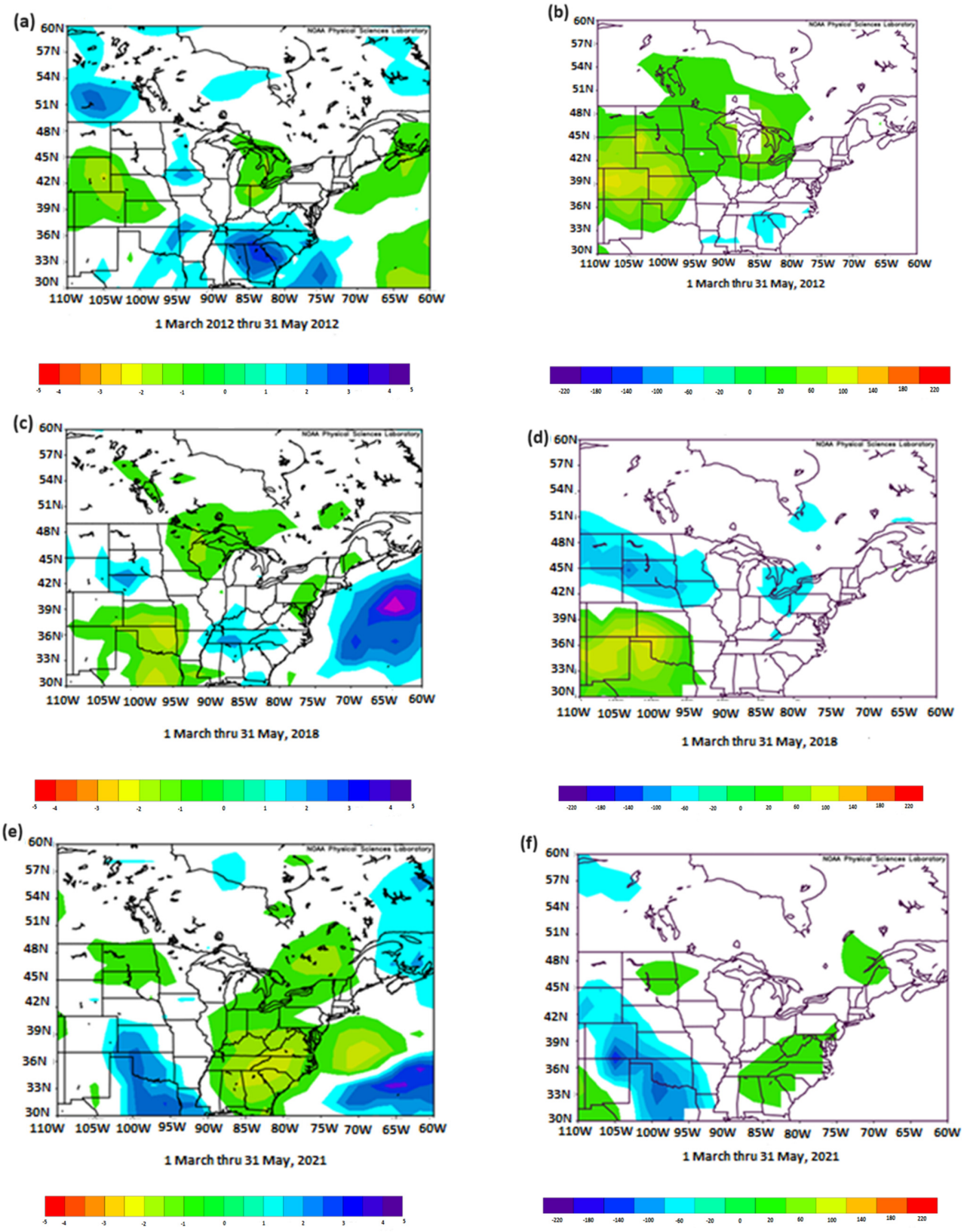

Figure 12. *Cont.*

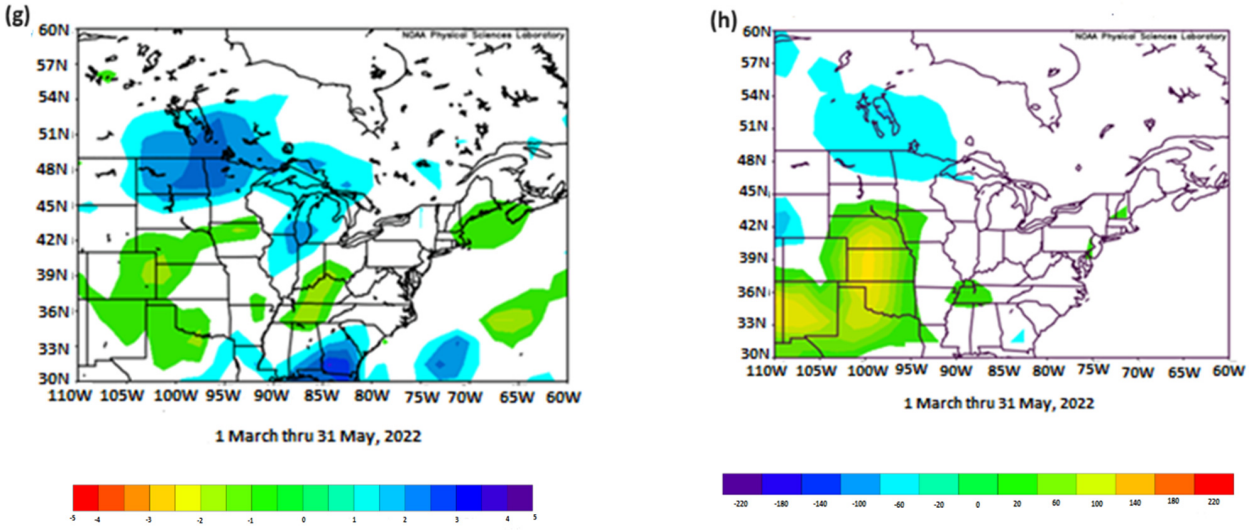

Figure 12. The spring (1 March to 31 May) season precipitation (mm day^{-1}) (**left**) and surface potential evaporation (W m^{-2}) (**right**) for (**a**,**b**) 2012, (**c**,**d**) 2018, (**e**,**f**) 2021, and (**g**,**h**) 2022.

For the summers of 2012 and 2022, there were areas that consisted of higher surface potential evaporation across much of the Midwest (Figure 13b,h), including much of the study region. The summers of 2018 and 2021 showcased negative values of surface potential evaporation across the Midwest and portions of the South in the US which were more similar to the spring values (Figure 12b,h). However, upon looking at the summers of 2018 and 2021, the areas of potential evaporation were the opposite of their spring patterns (Figures 12d,f and 13d,f).

During the spring of 2021 (Figure 12e), there were positive anomalies of surface precipitation indicating precipitation in abundance for portions of the Midwest and South, as shown via the areas of cool (blue and purple). Summer of 2012 (Figure 13a) showed negative values of surface precipitation anomalies indicating the development of strong drought ongoing in most of the Midwest and portions of the South. The summer of 2018 (Figure 13c) was a bit different in that there were areas of the Midwest and South that showed positive values of surface precipitation anomalies indicating less potential for widespread drought. The Great Lakes and extreme South endured negative values of surface precipitation anomalies showcasing areas of potential drought. Most of the South had positive values of surface precipitation anomalies for the summer of 2021 (Figure 13e) resulting in a year with less drought potential. Heavier precipitation was showcased across extreme portions of the South, shown in purple. This area of precipitation also went into portions of the Midwest and Northeast, including the eastern portion of the Great Lakes. Some southern states and northern Midwest areas had negative values of surface precipitation rate indicating local drought in the northwest portion of the study region. The entire Midwest endured drought conditions during the summer of 2022 (Figure 13g,h), with areas along the eastern coast enduring a drought as well. Portions of the South and Appalachians did have positive anomalies of rainfall.

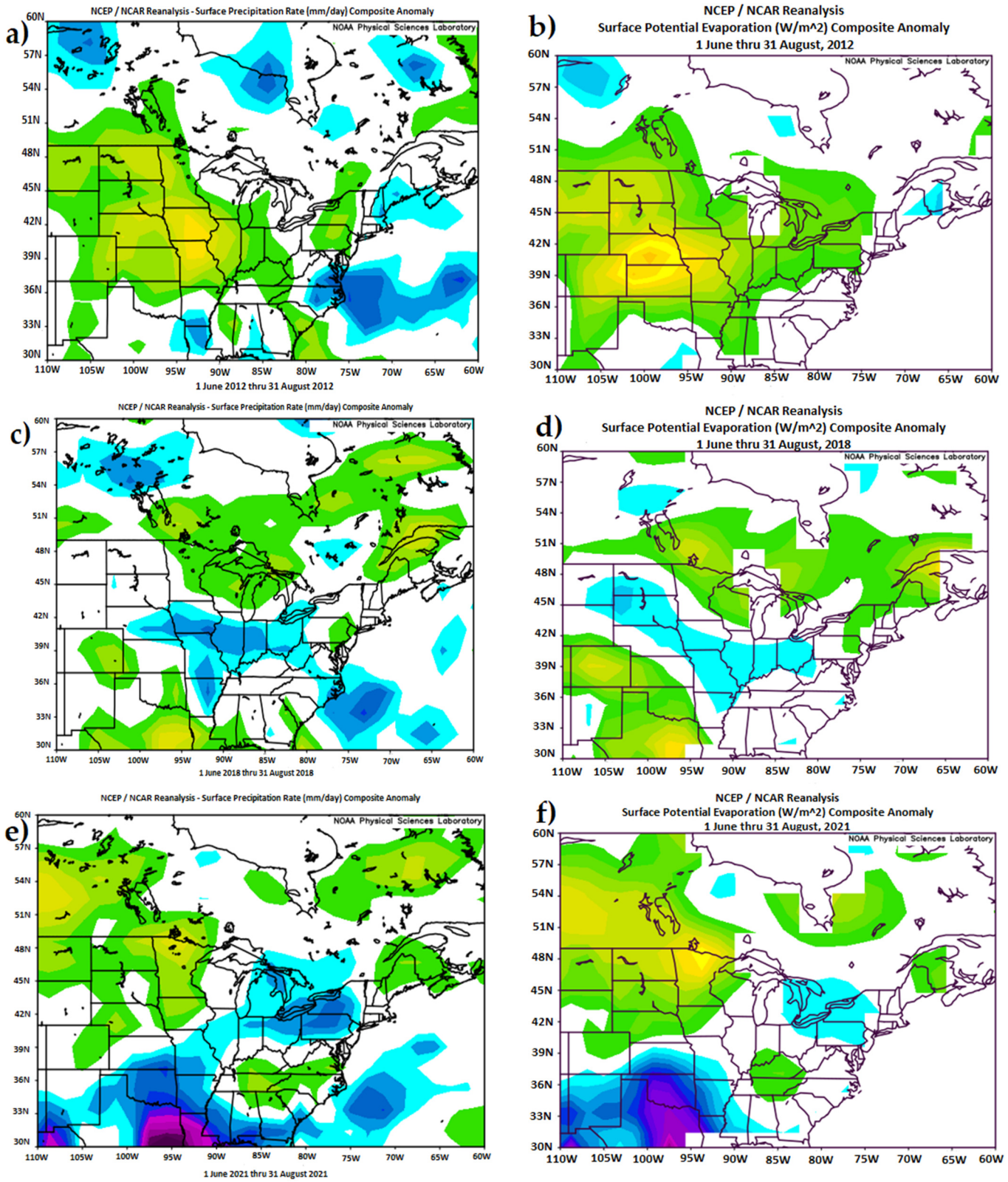

Figure 13. *Cont.*

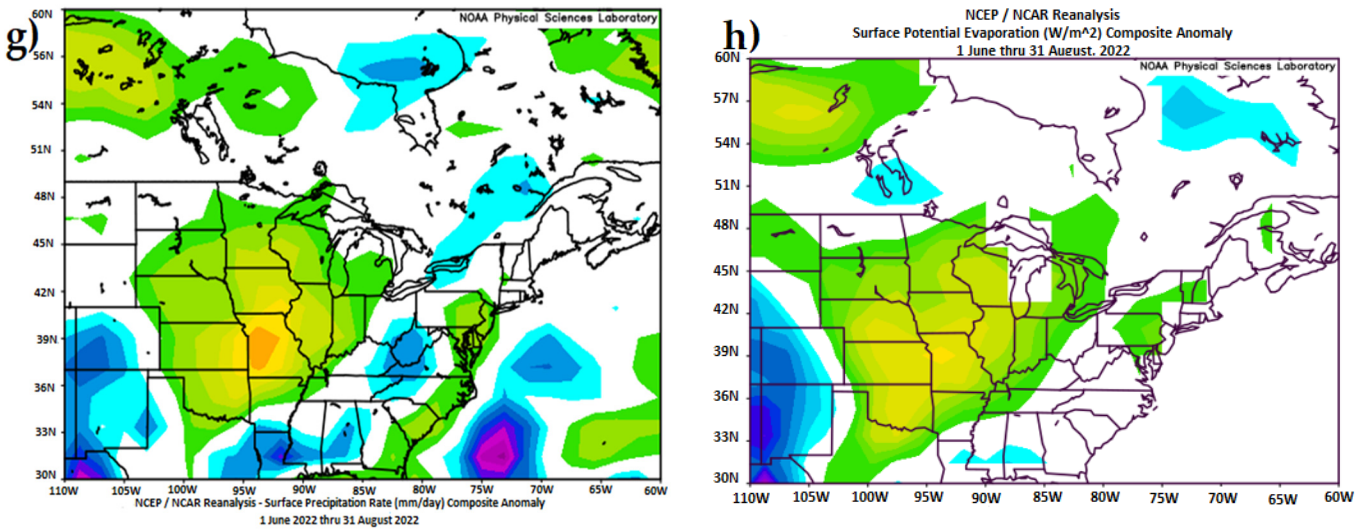

Figure 13. The summer (1 April to 30 June) season precipitation (mm day^{-1}) (**left**) and surface potential evaporation (W m^{-2}) (**right**) for (**a**,**b**) 2012, (**c**,**d**) 2018, (**e**,**f**) 2021, and (**g**,**h**) 2022. The color palette is the same as in Figure 12.

4. Discussion

In Section 3, it was noted that 2012 was among the hottest and driest summers across the study region except for the southernmost states. The summer of 2022 was qualitatively not as hot across the region and much of the region was dry, but not quite as dry across the region (Figure 3), but impacted a slightly larger region (Table 1). A comparison with two years of no significant drought region-wide was also conducted, and qualitatively, 2018 and 2021 were years that were not dry across the region (Table 1).

Firstly, Figure 12 will demonstrate that the study region shows areas of positive and negative precipitation anomalies, and no real pattern emerges to show differences between 2012 and 2022 versus 2018 and 2021. Also, in 2022, much of Missouri was above average for precipitation from March to May (Figure 12a and Table 5), and the state experienced regular rain events (not shown). However, three of the four years in Figure 12 show strong large-scale positive potential evaporation anomalies, except for 2021. Nonetheless, large-scale spring positive potential evaporation anomalies may be a precursor regardless of the precipitation.

Table 5. The NDI calculations for four cities in Missouri during spring and summer of 2012, 2018, 2021, and 2022.

Year	MCI	COU	STL	SGF
2012	−4.78/−3.79	−2.92/−3.26	−3.88/−2.80	−3.37/−2.30
2018	−1.17/−0.92	−1.32/−2.22	0.64/−1.20	−1.46/−0.84
2021	−0.47/−0.81	0.85/0.95	−0.89/0.44	1.48/−0.69
2022	0.47/−1.95	0.36/−2.04	−0.41/0.98	1.53/−1.93

Then, during summer (Figure 13), again, three of the four years including 2012 and 2022 showed widespread positive potential evaporation in the study region, with 2012 being the strongest. Qualitatively, 2022 was a little weaker than 2012, but covered much of the same region. For precipitation, 2022 shows the strongest and most widespread area of negative precipitation anomalies (Figure 13 and Table 1). During 2012, this negative summer precipitation anomaly was also widespread across the study region but was tempered in the southern part of the study region on 30–31 August 2012 by the remnants of Hurricane Isaac [52].

In order to corroborate the reliability of the methods used here, the recently published New Drought Index (NDI) was calculated following [53], using four National Weather Service (NWS) stations across Missouri in Springfield, Columbia, Saint Louis, and Kansas City. This NDI index uses a standardized anomaly of precipitation and temperature and here, spring and summer seasonal values were used. This index identifies meteorological drought similar to our methodology here. Missouri was located near the center of the study region and is a sub-region of interest to this group. Larger negative values indicate drier years since a positive temperature anomaly would be subtracted from a negative precipitation anomaly (see [53]) and uses observed station data.

The NDI values are shown in Table 5 and imply that the summer of 2012 was a more severe drought for both the spring and the summer seasons than 2022 for Missouri, but both summers were clearly worse than 2018 and 2021 overall. Table 1 implies the droughts were of comparable severity for the summer season, but regionwide. For spring 2022, the values were mainly positive due to the wetter spring (Figure 14a). For 2018 and 2021, the NDI values were generally closer to zero and a mix of positive and negative values. Only one station in central Missouri showed drier conditions locally in 2018, and in 2022, one station showed a positive value as the result of a 250 mm rainfall in 24 hours during July. Thus, the NDI and the index used here produced similar qualitative results even though these indexes may give different quantitative results using different study regions and data with different resolution, and this has been shown in many studies previously (e.g., [54,55]).

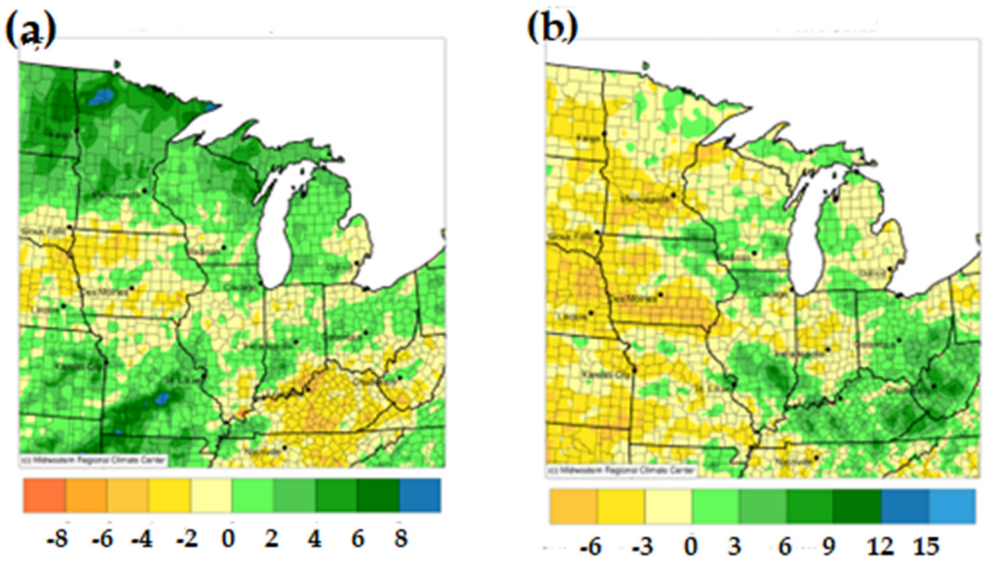

Figure 14. The precipitation anomalies for (**a**) spring (1 March–31 May 2022, inches) and (**b**) summer (1 June–31 August 2022, inches). Source: [56].

An examination of the 500 hPa summer height anomalies (Figure 10) showed strong positive height anomalies over the west US and into the central US and a negative AO index for the summer season (Table 2), which is consistent with drought years as demonstrated by [3]. However, [57] posited that summer season ridging will occur annually over the continental USA, but that the year-to-year differences were mainly in the location, amplitude, and intensity. In Figure 10, the positive (negative) height anomalies over Canada (USA) in 2018 and 2021 which were not drought years imply more zonal flow as indicated by positive values for the AO during the summer (Table 2). Thus far, there are differences in the flow pattern and surface character for North America during drought years versus non-drought years as established by [3], and 2022 is consistent with those results, but also numerous other studies (e.g., [24,58–63]).

The second question addressed here is could the drought of 2022 (or any drought year) be anticipated using surface conditions, blocking, or IE? Previous studies established a lack

of summer season blocking over the East Pacific region, and that any of these blocking events would be weak [3]. That was the case for summer 2022, which experienced one weak event over the East Pacific (Table 4). The non-drought years here did experience more than one East Pacific blocking, and these were of typical strength for the season and region [36,38]. However, [3] showed that spring seasons that precede dry summers would also be associated with weaker and less upstream blocking from North America. In 2022, this was not the case (Table 3). In fact, there was more blocking in the East Pacific, which is characteristic of wetter summer conditions.

Finally, here, the IE diagnostic was applied in order to determine whether or not a change in the regional or NH flow regime could be identified with the onset of the summer regime, and thus, the 2022 drought. Newberry et al. [18] argued that the onset of the summer season regime for Missouri could be detected by examining the change in the local temperatures (more consistently warm), a northward shift in the 500 hPa jet, and precipitation frequency and intensity. They also used IE to argue that the summer season flow regimes are associated with weaker enstrophy. They noted that some of these seasonal changes could be quite abrupt, while others were more gradual. Est et al. [30] investigated the question of whether the onset of a more spring-like regime could be identified using the occurrence of IE maxima. Then, ref. [18] identified 3 and 7 June as the onset of the summer season regime for Missouri and the surrounding region in 2012 and 2022, respectively.

Figure 11 shows that after 5 June 2022, the NH IE decreased and never recovered. Applying the methodology of [18] would demonstrate that for the Missouri region, the temperature and precipitation regime was very different before and after 7 June 2022, and this was also true regionwide (Figure 14). Given that spring was quite wet, drought conditions did not begin to be displayed regionwide until early July 2022 (Figure 8a). For 2012, the IE decreased after 10 June and this was a little later than 3 June, but consistent with the change in the 500 hPa height criterion found in [18], which indicated the jet stream had moved poleward for much of the region.

Additionally, [29,30] show that the primary NH teleconnection indexes (e.g., Figure 9) changed their characteristic slope in association with the maximum in IE. In 2022, all three indexes (AO, NAO, and PNA) show strong sign changes in their slope during early June (5 June). The AO and NAO change from a negative slope (-0.22 and -0.08) during the second half of May up to 5 June, to a positive slope (0.18 and 0.06) following the 5th, and up to the 20 June 2022. The PNA turned from a positive slope (0.03) before 5 June to a negative slope following this date (-0.10). In 2012, the changes in the slope sign are the same as 2022 for all three indexes before and after 3 June.

Also, [3] posited that dry springs generally associated positive AO and NAO but negative PNA indexes, but extreme dry summers were a bit different in that all three indexes will generally be negative. As shown in Table 3 and [49], the AO and NAO correlate positive and strongly, while the PNA correlates negatively by comparison in general. During these dry summer seasons; however, all three indexes were negative in 2012 and other summers (see [3]), but this was not the case in 2022.

Thus, it can be shown in retrospect, that the onset of the 2022 drought can be identified as early June given the occurrence of the NH IE maximum and change in teleconnections. Also, the spring and summer of 2012 and 2022 were similar in several respects including a large-scale region of potential evaporation over the study region and adjacent regions and strong, widespread areas of positive potential evaporation and negative precipitation anomalies resulting in large negative quantities of precipitation and evaporation. The summer season 500 hPa height anomalies over North America and the lack of frequent upstream Pacific blocking were similar as well. However, the spring of 2022 did show frequent upstream spring blocking and a different summer season teleconnection index regime than summer 2012. In retrospect, it is not clear that the drought of 2022 could have been anticipated until and in spite of the occurrence of the NH IE maximum. Lastly, 2012 and 2022 differ from 2018 and 2021 in a similar fashion as proposed by [3]. Yet, these results

show that drought may be anticipated with reasonable certainty based on the surface and upper air characteristics of atmospheric variables and quantities found and examined here.

5. Conclusions

Drought has always been an issue for the entire world, and it will continue to be an issue for many years to come. Previous studies noted that dry summers were associated with different large-scale flow regimes over North America from wetter summers and optimal surface conditions, but these studies also noted that spring was not necessarily an indicator of summer drought over North America. In this work, the spring and summer of 2022 were examined to determine how similar the large-scale flow and surface conditions were to those in 2012, but different from 2018 and 2021, which were not considered drought years.

During the spring of 2022, the East Pacific region was very active in terms of blocking, and this is more characteristic of wetter summers. However, summer 2022 was like the summer of 2012 in that there were strong positive height anomalies over the plains with one relatively weak blocking event occurring in the East Pacific. For summer 2022, it appears that the monthly NAO and PNA are both the same sign similar to but of opposite sign to 2012.

Ridging is typically associated with years that endured drought and that is the case for the summers of 2012 and 2022. Previous work showed that all summers are associated with ridging over the USA and that the main year-to-year difference is in the amplitude, intensity, and location. In the United States for the summers of 2018 and 2021, the flow was relatively more zonal over most of the United States, which is not like the drought years of 2012 and 2022, which were more amplified.

Finally, the surface conditions showed large-scale regions of higher spring season potential evaporation during the two drought years and 2018. However, for the two dry summers, these regions of potential evaporation became larger and stronger, while there were concomitant shortfalls in precipitation. Thus, it is clear that while potential evaporation during the spring of 2022 may have foreshadowed the summer drought, the precipitation and large-scale flow patterns, particularly the occurrence of blocking, produced mixed results. In spite of this, the large-scale conditions for the very dry summer of 2022 were similar to those found in other studies for previous years (e.g., 2012) within the area of study. The conditions for the non-drought summers of 2018 and 2021 were quite different. A recently published drought index qualitatively corroborated the differences between 2012 and 2022 versus 2018 and 2021.

Lastly, the IE diagnostic employed in previous work may have identified the change in flow regime over North America that led to drought. There were maxima in both years during early June when the precipitation and temperature regimes changed over the region. These IE maxima were also associated with changes in the slope for the daily time series of the major NH teleconnection indexes as in previous studies.

Additional study is warranted in order to confirm the results, including (a) the potential to use the results of block occurrence and IE changes to anticipate future drought, (b) the application of these results to other areas on the globe, or (c) using different drought indexes.

Author Contributions: Conceptualization, A.R.L., P.E.G. and I.G.S.; methodology, S.M.W., A.R.L. and I.G.S.; software, S.M.W. and A.R.L.; validation, All; formal analysis, S.M.W., P.E.G. and A.R.L.; investigation, S.M.W.; resources, All; data curation, S.M.W. and A.R.L.; writing—original draft preparation, S.M.W. and A.R.L.; writing—review and editing, All; visualization, S.M.W. and A.R.L.; supervision, A.R.L., N.A. and S.H.; project administration, A.R.L., N.A. and S.H.; funding acquisition, A.R.L., N.A. and S.H. All authors have read and agreed to the published version of the manuscript.

Funding: This work was supported in part by the U.S. Department of Agriculture (USDA)—Agricultural Research Service Non-Assistance Cooperative Agreement. Mention of trade names or commercial products in this publication is solely for the purpose of providing specific information and does not imply recommendation or endorsement by the U.S. Department of Agriculture. The USDA is an equal opportunity provider and employer.

Institutional Review Board Statement: Not applicable.

Informed Consent Statement: Not applicable.

Data Availability Statement: The data are available through the Global Climate Change Laboratory at the University of Missouri [36].

Acknowledgments: The authors are grateful for the time and effort given by the anonymous reviewers whose contributions greatly strengthened this manuscript.

Conflicts of Interest: The authors declare no conflict of interest.

References

1. Intergovernmental Panel on Climate Change (IPCC). Climate Change 2013: The Physical Scientific Basis. 2013. Available online: http://www.ipcc.ch (accessed on 8 June 2021).
2. National Weather Service—National Oceanic and Atmospheric Administration. 2022. Available online: https://www.weather.gov/bmx/kidscorner_drought (accessed on 20 December 2022).
3. Lupo, A.R.; Kononova, N.K.; Semenova, I.G.; Lebedeva, M.G. A Comparison of the characteristics of extreme drought during the late 20th and early 21st centuries over Eastern Europe, Western Russia, and Central North America. *Atmosphere* **2021**, *12*, 1033. [CrossRef]
4. NOAA—NIDIS, 2022: Defining Drought. Available online: https://www.drought.gov/what-is-drought/drought-basics (accessed on 2 December 2022).
5. Ahrens, C.D.; Henson, R. *Meteorology Today: An Introduction to Weather, Climate, and the Environment*, 11th ed.; Cengage Learning: Boston, MA, USA, 2000.
6. American Meteorological Society (AMS). Drought. 2013. Available online: https://www2.ametsoc.org/ams/index.cfm/aboutams/ams-statements/statements-of-the-ams-in-force/drought/ (accessed on 28 July 2021).
7. Cherenkova, Y.A. Quantitative evaluation of atmospheric drought in federal districts of the European Russia. *Proc. Russ. Acad. Sci. Geogr. Ser.* **2013**, *6*, 76–85. (In Russian)
8. Zuo, D.; Cai, S.; Xu, Z.; Peng, D.; Kan, G.; Sun, W.; Pang, B.; Yang, H. Assessment of meteorological and agricultural droughts using in-situ observations and remote sensing data. *Agric. Water Manag.* **2019**, *222*, 129–138. [CrossRef]
9. Stefanidis, S.; Rossiou, D.; Proutsos, N. Drought severity and trends in a Mediterranean oak forest. *Hydrology* **2023**, *10*, 167. [CrossRef]
10. Mohammadi, B. Modeling various drought time scales via a merged Artificial Neural Network with a Firefly Algorithm. *Hydrology* **2023**, *10*, 58. [CrossRef]
11. Allen, R.A.; Fletcher, R.; Holmboe, J.; Namias, J.; Willett, H.C. *Report on an Experiment in Five-Day Weather Forecasting*; Massachusetts Institute of Technology and Woods Hole Oceanographic Institution: Woods Hole, MA, USA, 1940.
12. Namias, J. The great pacific anticyclone of winter 1949–1950: A case study in the evolution of climatic anomalies. *J. Meteor.* **1951**, *8*, 251–261. [CrossRef]
13. Wallace, J.M.; Gutzler, D.S. Teleconnections in the geopotential height field during the Northern Hemisphere winter. *Mon. Weather Rev.* **1981**, *109*, 784–812. [CrossRef]
14. Kung, E.C.; Chern, J.-G. Prevailing anomaly patterns of the global sea surface temperatures and tropospheric responses. *Atmosfera* **1995**, *8*, 99–114.
15. Birk, K.; Lupo, A.R.; Guinan, P.E.; Barbieri, C.E. The interannual variability of midwestern temperatures and precipitation as related to the ENSO and PDO. *Atmosfera* **2010**, *23*, 95–128.
16. Lupo, A.R.; Kelsey, E.P.; Weitlich, D.K.; Davis, N.A.; Market, P.S. Using the monthly classification of global SSTs and 500 hPa height anomalies to predict temperature and precipitation regimes one to two seasons in advance for the mid-Mississippi region. *Nat. Weather Dig.* **2008**, *32*, 11–33.
17. Lupo, A.R.; Mokhov, I.I.; Chendev, Y.G.; Lebedeva, M.G.; Akperov, M.; Hubbart, J.A. Studying summer season drought in Western Russia. *Adv. Meteorol.* **2014**, *2014*, 942027. [CrossRef]
18. Newberry, R.G.; Lupo, A.R.; Jensen, A.D.; Zalipynis, R.A. An analysis of the spring-to-summer transition in the west central plains for application to long range forecasting. *Atmos. Clim. Sci.* **2016**, *6*, 375–393. [CrossRef]
19. Nunes, M.J.; Lupo, A.R.; Lebedeva, M.G.; Chendev, Y.G.; Solovyov, A.B. The occurrence of extreme monthly temperatures and precipitation in two global regions. *Pap. Appl. Geog.* **2017**, *3*, 143–156. [CrossRef]
20. Renken, J.S.; Herman, J.J.; Brandshaw, T.R.; Market, P.S.; Lupo, A.R. The utility of the Bering Sea and East Asia Rules in long-range forecasting. *Adv. Meteor.* **2017**, *2017*, 1765428. [CrossRef]
21. Jiang, X.; Lau, N.-C. Intraseasonal teleconnection between North American and Western North Pacific monsoons with 20-day time scale. *J. Clim.* **2008**, *21*, 2664–2679. [CrossRef]
22. Zhao, P.; Cao, Z.; Chen, J. A summer teleconnection pattern over the extratropical Northern Hemisphere and associated mechanisms. *Clim. Dyn.* **2010**, *35*, 523–534. [CrossRef]
23. Wang, Y.; Lupo, A.R.; Qin, J. A response in the ENSO cycle to an extratropical forcing mechanism during the El Nino to La Nina transition. *Tellus Ser. A Dyn. Meteorol. Oceanogr.* **2013**, *65*, 22431. [CrossRef]

24. Henson, C.B.; Lupo, A.R.; Market, P.S.; Guinan, P.E. ENSO and PDO-related climate variability impacts on Midwestern United States crop yields. *Int. J. Biometeorol.* **2017**, *61*, 857–867. [CrossRef]
25. Cherenkova, E.; Semenova, I.; Bardin, M.; Zolotokrylin, A.N. Drought and grain crop yields over the East European Plain under influence of quasibiennial oscillation of global atmospheric processes. *Int. J. Atmos. Sci.* **2015**, *2015*, 932474. [CrossRef]
26. Athar, H.; Lupo, A.R. Scale and stability analysis of blocking events from 2002–2004: A case study of an unusually persistent blocking event leading to a heat wave in the Gulf of Alaska during August 2004. *Adv. Meteor.* **2010**, *2010*, 610263. [CrossRef]
27. Jensen, A.D.; Lupo, A.R.; Mokhov, I.I.; Akperov, M.G.; Reynolds, D.D. Integrated regional enstrophy and block intensity as a measure of Kolmogorov Entropy. *Atmosphere* **2017**, *8*, 237. [CrossRef]
28. Jensen, A.; Lupo, A.R.; Mokhov, I.I.; Akperov, M.G.; Sun, F. The dynamic character of Northern Hemisphere flow regimes in a near term climate change projection. *Atmosphere* **2018**, *9*, 27. [CrossRef]
29. Klaus, E.M.; Market, P.S.; Lupo, A.R.; Bodner, M.J.; Kastman, J.S. Projecting Northern Hemisphere flow regime transition using integrated enstrophy. *Atmosphere* **2000**, *11*, 915. [CrossRef]
30. Est, M.A.; Mount, S.; Steward, C.A.; Lebedeva, M.G.; Lupo, A.R. Northern Hemisphere flow regime transitions, blocking, and the onset of spring in the central USA. *Meteorology* **2022**, *1*, 19.
31. NOAA Physical Sciences Laboratory: NCEP—NCAR Reanalysis. 2022. Available online: https://psl.noaa.gov/data/gridded/data.ncep.reanalysis.html (accessed on 20 December 2022).
32. Kalnay, E.; Kanamitsu, M.; Kisler, R.; Collins, W.; Deaven, D.; Gandin, L.; Iredell, M.; Saha, S.; White, G.; Woolen, J.; et al. The NCEP/NCAR 40-year reanalysis project. *Bull. Am. Meteorol. Soc.* **1996**, *77*, 437–471. [CrossRef]
33. Kistler, R.; Kalnay, E.; Collins, W.; Saha, S.; White, G.; Wollen, J.; Chelliah, M.; Ebisuzaki, W.; Kanamistu, M.; Kousky, V.; et al. The NCEP-NCAR 50-year reanalyses: Monthly means CD-ROM and documentation. *Bull. Am. Meteorol. Soc.* **2001**, *82*, 247–268. [CrossRef]
34. Bao, X.; Zhang, F. Evaluation of NCEP-CFSR, NCEP-NCAR, ERA-interim, and ERA-40 reanalysis datasets against independent sounding observations over the Tibetan Plateau. *J. Clim.* **2013**, *26*, 206–214. [CrossRef]
35. He, W.-P.; Zhao, S.-S. Assessment of the quality of NCEP-2 and CFSR reanalysis daily temperature in China based on long-range correlation. *Clim. Dyn.* **2018**, *50*, 493–505. [CrossRef]
36. University of Missouri Blocking Archive. 2022. Available online: http://weather.missouri.edu/gcc/ (accessed on 2 November 2022).
37. Lupo, A.R. Atmospheric Blocking Events: A Review. *Ann. N. Y. Acad. Sci.* **2020**, *1504*, 5–24. [CrossRef]
38. Lupo, A.R.; Jensen, A.D.; Mokhov, I.I.; Timazhev, A.V.; Eichler, T.; Efe, B. Changes in global blocking character during the most recent decades. *Atmosphere* **2019**, *10*, 92. [CrossRef]
39. Mappr, 2023: United States Regions Map. Available online: https://www.mappr.co/political-maps/us-regions-map/ (accessed on 1 September 2023).
40. NCDC—NOAA: June–August 2012 Statewide Ranks—Precipitation. Available online: https://www.ncdc.noaa.gov/sotc/service/national/Statewideprank/201206-201208.gif (accessed on 20 December 2022).
41. NCDC—NOAA: June–August 2012 Statewide Ranks—Temperature. Available online: https://www.ncdc.noaa.gov/sotc/service/national/Statewidetrank/201206-201208.gif (accessed on 20 December 2022).
42. National Centers for Environmental Information: Annual 2012 National Climate Report. Available online: https://www.ncdc.noaa.gov/sotc/national/201213 (accessed on 20 December 2022).
43. NCDC—NOAA: January–December 2012 Statewide Ranks—Precipitation. Available online: https://www.ncdc.noaa.gov/sotc/service/national/Statewideprank/201201-201212.gif (accessed on 20 December 2022).
44. NCDC—NOAA: January–December 2012 Statewide Ranks—Temperature. Available online: https://www.ncdc.noaa.gov/sotc/service/national/Statewidetrank/201201-201212.gif (accessed on 20 December 2022).
45. National Centers for Environmental Information: Annual 2018 National Climate Report. Available online: https://www.ncei.noaa.gov/access/monitoring/monthly-report/national/201813 (accessed on 5 January 2023).
46. National Centers for Environmental Information: Annual 2021 National Climate Report. Available online: https://www.ncei.noaa.gov/access/monitoring/monthly-report/national/202113 (accessed on 5 January 2023).
47. National Center for Environmental Information: Annual 2022 National Climate Report. Available online: https://www.ncei.noaa.gov/access/monitoring/monthly-report/national/202213 (accessed on 5 January 2023).
48. U.S. Drought Monitor Maps. 2023. Available online: https://droughtmonitor.unl.edu/CurrentMap.aspx (accessed on 23 June 2023).
49. Lebedeva, M.G.; Lupo, A.R.; Chendev, Y.G.; Krymskaya, O.V.; Solovyev, A.B. Changes in the atmospheric circulation conditions and regional climatic characteristics in two remote regions since the mid-20th century. *Atmosphere* **2019**, *10*, 11. [CrossRef]
50. National Weather Service—Climate Prediction Center, 2022: AAO, AO, NAO, PNA. Available online: https://www.cpc.ncep.noaa.gov/products/precip/CWlink/daily_ao_index/teleconnections.shtml (accessed on 30 December 2022).
51. American Meteorological Society—Glossary of Meteorology: Enstrophy. Available online: https://glossary.ametsoc.org/wiki/Enstrophy (accessed on 10 May 2023).
52. National Hurricane Center (USA). 2023. Available online: https://www.nhc.noaa.gov/data/ (accessed on 22 June 2023).
53. Bonacci, O.; Bonacci, D.; Bonacci, T.R.; Vrsalovic, A. Proposal of a new method for drought analysis. *J. Hydrol. Hydromech.* **2023**, *71*, 100–110. [CrossRef]

54. Mitra, S.; Srivastava, P. Spatiotemporal variability of meteorological droughts in southeastern USA. *Nat. Hazards* **2017**, *86*, 1007–1038. [CrossRef]
55. Barnard, D.M.; Germino, M.J.; Bradford, J.B.; O'Connor, R.C.; Andrews, C.M.; Shriver, R.K. Are drought indices and climate data good indicators of ecologically relevant soil moisture dynamics in drylands? *Ecol. Indic.* **2021**, *133*, 108379. [CrossRef]
56. Midwest Regional Climate Center. 2023. Available online: https://mrcc.purdue.edu/CLIMATE/index.jsp (accessed on 28 June 2023).
57. Lupo, A.R.; Smith, N.B.; Guinan, P.E.; Chesser, M.D. The climatology of Missouri region dew points and the relationship to ENSO. *Nat. Weather Dig.* **2012**, *36*, 82–91.
58. Kahya, E.; Dracup, J.A. U.S. streamflow patterns in relation to the El Niño/Southern Oscillation. *Water Resour. Res.* **1993**, *29*, 2491–2503. [CrossRef]
59. Dracup, J.A.; Kahya, E. The relationships between US streamflow and La Niña events. *Water Resour. Res.* **1994**, *30*, 2133–2141. [CrossRef]
60. Ting, M.; Wang, H. Summertime U.S. Precipitation Variability and Its Relation to Pacific Sea Surface Temperature. *J. Clim.* **1997**, *10*, 1853–1873. [CrossRef]
61. Mo, K.C.; Schemm, J.E. Relationships between ENSO and drought over the southeastern United States. *Geophys. Res. Lett.* **2008**, *35*, L15701. [CrossRef]
62. Mo, K.C.; Schemm, J.E. Drought and persistent wet spells over the United States and Mexico. *J. Clim.* **2008**, *21*, 980–994. [CrossRef]
63. Rajagopalan, B.; Cook, E.; Lall, U.; Ray, B.K. Spatiotemporal Variability of ENSO and SST Teleconnections to Summer Drought over the United States during the Twentieth Century. *J. Clim.* **2000**, *13*, 4244–4255. [CrossRef]